INDOOR AIR 2020
The 16th Conference of the International Society of Indoor Air Quality & Climate
ONLINE | From November 1, 2020
Paper ID ABS-0224

Development of autonomic regulation model for cardiovascular system simulations

Tomonobu Goto[1*], Hiroto Sakamoto[2], Atsushi Utsunomiya[1], Kenta Shishikura[1]

[1] Tohoku University, Japan
[2] Maeda Corporation, Japan

[*]*Corresponding email: t-goto@sabine.pln.archi.tohoku.ac.jp*

SUMMARY
In order to evaluate health risks under sever thermal environments, we are developing a new human model that can predict BP and BFR, as well as body temperature. In this study, we developed one of the sub-models for our human model, i.e. autonomic regulation model, which predicts human responses on vasomotor and cardiac activities for thermoregulation and baroreflex. We also conducted some simulations by using the autonomic regulation model combined with our previously developed model of cardiovascular system. The results showed that the simulations reproduced reasonably the actual BP and BFR under four different thermal and postural conditions, i.e. 18°C, 28°C, 40°C-supine and 28°C-standing. Only in the 18°C-supine case, there was a substantial problem on the BP simulation, however, it will be solved by the incorporation of more precise vasomotor activity.

KEYWORDS
Thermal environment; Health risk; Human model; Blood pressure; Blood flow rate

1 INTRODUCTION
Severe thermal environments can cause human health problems, such as heat illness, cerebral stroke, and heart attack, and the incidence of these health issues is increasing as the population ages in Japan (Ministry of the environment government of Japan, 2018; Tokyo metropolitan institute of gerontology, 2013). In the characterization of these health issues, changes in the body temperature, blood pressure (BP), and blood flow rate (BFR) are the key factors. In addition, these health problems are affected not only by thermal environments, but also by individual behaviors (posture and activity level), physical constitutions (size, composition), and predispositions (pre-existing disorder, age, gender, heredity). In other words, the risks of these health problems are attributed to the combined effect of the abovementioned factors.

Numerical simulation with human thermophysiological models is a useful method to evaluate the health risks induced by severe thermal environments and to perceive the mechanisms of occurrence of such health problems. However, the BFR predictions in the existing models are not based on direct measurements of BFR and not validated sufficiently, because those models were developed mainly for body temperature predictions. Moreover, the existing models cannot predict BP, because the vessels in those models are neglected or do not represent the actual vessel configurations. Thus, there are no models presently available to predict BP and BFR.

For the above reasons, we have been developing a new human model, which can predict not only body temperature, but also BP and BFR (Figure 1). In our previous studies, we had developed the physical models, i.e. thermal network model and cardiovascular model (Sakamoto et al., 2015; Goto et al., 2017; Goto et al., 2018). In the present study, we developed a part of the autonomic regulation model such as vasomotor and cardiac activities for thermoregulation and baroreflex. In addition, we conducted simulations under four different thermal and postural conditions by using the autonomic regulation model combined with the cardiovascular model.

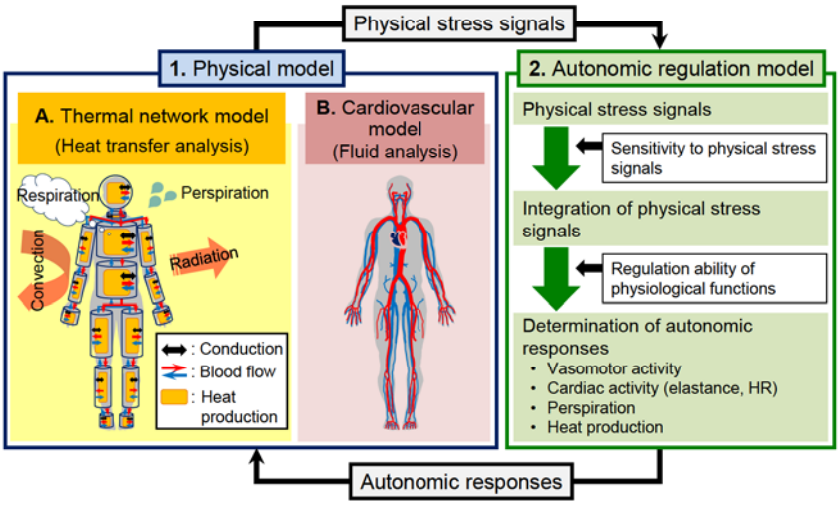

Figure 1. Schematic of new thermophysiological human model

2 METHODS

2.1 CARDIOVASCULAR MODEL

Our cardiovascular model was developed based on Liang et al. (2009). As shown in Figure 2, the model consists of a one-dimensional (1-D) model and lumped parameter (0-D) model. The 1-D model describes the blood flow phenomena in an arterial tree. The arterial tree in our model consists of 69 arteries. The 0-D model describes the blood flow phenomena in the remaining cardiovascular system, i.e., peripheral circulations, venae cavae, heart, and pulmonary circulation. The typical peripheral circulation in our model is shown in Figure 3. Basically, each segment is represented by the viscosity resistance (R), inertial resistance (L), and compliance (C). The heart and pulmonary circulation in our model are shown in Figure 4. The governing equations of the cardiovascular model are shown in Table 1.

The quantitative values for the model parameters should be altered according to the individual characteristics and physiological states of the target human. We defined the physiological state under the thermally neutral and supine condition as “basic physiological state”, and also defined the setting of the model parameter values for the basic physiological state as “basic parameter setting”. Therefore, individual characteristics can be taken into account by making differences in the basic parameter setting, and changing physiological state can be reflected as the adjustment of the values from the basic parameter setting. In the present study, the basic parameter setting was determined based on the measurements in our previous studies (Sakamoto et al., 2015; Goto et al., 2017; Goto et al., 2018).

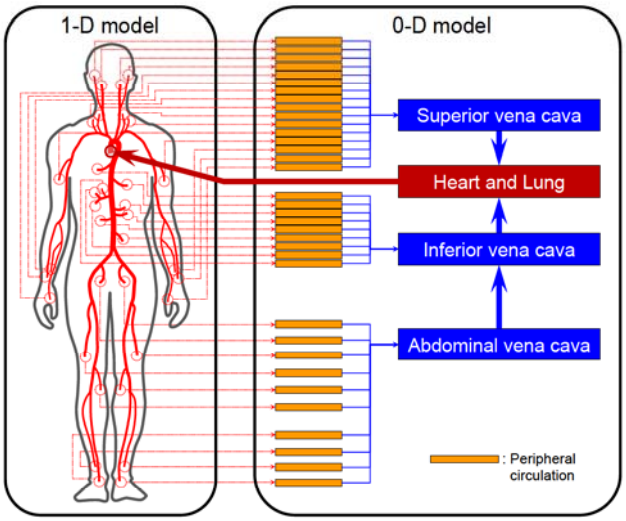

Figure 2. Schematic of cardiovascular model

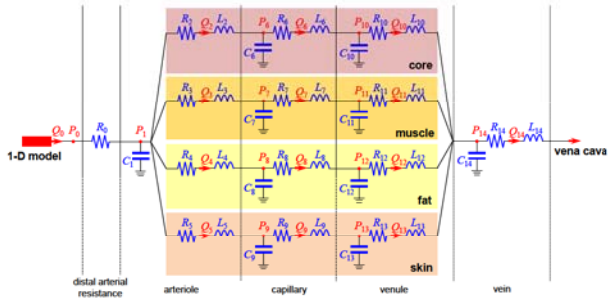

Figure 3. Typical peripheral circulation in 0-D model

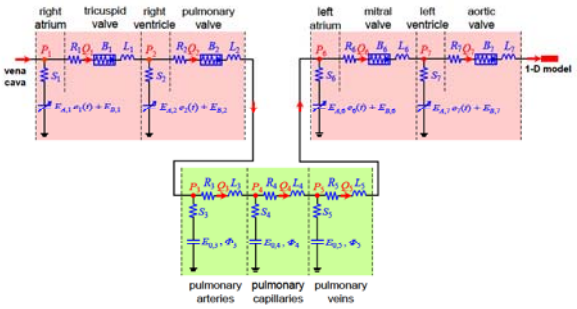

Figure 4. Heart and pulmonary circulation in 0-D model

Table 1. Equations of cardiovascular model

1-D model

$$\frac{\partial A}{\partial t}+\frac{\partial Q}{\partial x}=0, \qquad \frac{\partial Q}{\partial t}+\frac{\partial}{\partial x}\left(\frac{Q^2}{A}+\frac{A}{\rho}P+gAH\right)+\frac{2\pi r\nu}{\delta}\frac{Q}{A}=0, \qquad P=\frac{Eh}{r_0(1-\sigma^2)}\left(\sqrt{\frac{A}{A_0}}-1\right)$$

0-D model

$$\frac{dV_i}{dt}=Q_{up}-Q_i, \qquad P_i-P_{dw}=Q_iR_i+Q_i^2B_i+L_i\frac{dQ_i}{dt}+\rho gH, \qquad P_i=\frac{V_i}{C_i}\ \text{(for peripheral circulation and vena cava)},$$

$$P_i=\left(E_{A,i}e_i(t)+E_{B,i}\right)V_i+S_i\frac{dV_i}{dt}\ \text{(for heart)}, \qquad P_i=E_{0,i}\Phi_i\exp\left(\frac{V}{\Phi_i}\right)+S_i\frac{dV_i}{dt}\ \text{(for pulmonary circulation)}$$

2.2 AUTONOMIC REGULATION MODEL

In the present study, we dealt with only vasomotor and cardiac activities, although our autonomic regulation model should predict the responses on perspiration and heat production as well. The vasomotor and cardiac activities occur not only for body temperature control but also for blood pressure control. Thus, we developed the autonomic regulation model to simulate both of these controls.

It is known that arterioles play the main role of the vasomotor activity for thermoregulation. Thus, we applied the equations in Table 2 to describe the relationship between the viscosity resistances (R) of arterioles and thermal stress signals. Thermal stress signals *STRIC* and *DILAT* are the integrated signals of whole body, which are calculated from head core and skin temperatures in the same manner as Stolwijk (1971). The coefficients $B_{stric,i}$ and $B_{dilat,i}$ are specific values of each arteriole. Theoretically, R is inversely proportional to the square of

vessel cross-sectional area, while inertial resistance (L) and compliance (C) are inversely and directly proportional to the cross-sectional area, respectively. Therefore, the L and C of each arteriole were considered to vary as described in Table 2. It is also known that arteriovenous anastomoses (AVAs) in hands and feet pass large amount of blood from arterioles directly to venules when body temperature is high. Since the AVAs activity can be translated into the changes in the resistances (R) of capillaries and venules, the same equation as arterioles was applied to the capillaries and venules only in hands and feet.

Changes of BP are caused by the vasomotor activities of thermoregulation, and more obviously by posture changes. The autonomic nerve system maintains the BP close to the normal level, which is known as baroreflex. The changes of BP are detected by baroreceptors that are mainly located in the wall of carotid sinus and aortic arch (Guyton and Hall, 2005). When a decrease in BP is detected by them, the central nerve system induces a decrease in the venous system volume, an increase in the heart rate and cardiac contractility, and an increase in the arteriole resistance. When an increase in BP is detected, vice versa. In order to prevent the complexity of the model, only the baroreflex responses of venous system and heart were considered in the present study. The vasomotor activities of venous system can be translated into the changes of the compliance (C), and the changes of the cardiac contractility can be translated into the changes of the active elastance (E_A). Thus, we applied the equations in Table 2 to describe the relationships between the BP and baroreflex responses.

Table 2. Equations of autonomic regulation model (vasomotor and cardiac activities)

Thermoregulation

$$DILAT = C_{dil}\left(T_{cr} - T_{cr,set}\right) + S_{dil}\left(\overline{T}_{sk} - \overline{T}_{sk,set}\right), \qquad STRIC = -C_{con}\left(T_{cr} - T_{cr,set}\right) - S_{con}\left(\overline{T}_{sk} - \overline{T}_{sk,set}\right),$$

$$VASO_i = \frac{1 + B_{stric,i} \cdot STRIC}{1 + B_{dilat,i} \cdot DILAT}, \qquad R_i = R_{i,basic} \times VASO_i, \qquad L_i = L_{i,basic} \times VASO_i^{0.5}, \qquad C_i = C_{i,basic} / VASO_i^{0.5}$$

Baroreflex

$$BARO = 1 + B_{baro,a}\left\{\frac{1}{1 + \exp\left[-B_{baro,s}\left(P_{ar} - P_{ar,set}\right)\right]} - 0.5\right\},$$

$$C_i = C_{i,basic} \times BARO, \qquad E_{A,i} = E_{A,i,basic} / BARO, \qquad HR = HR_{basic} / BARO$$

2.3 SIMULATION

In order to validate the autonomic regulation model, some simulations were conducted by using this model combined with the cardiovascular model. The simulated cases were selected as shown in Table 3, which corresponded to the experimental cases in our previous studies (Sakamoto et al., 2015; Goto et al., 2017; Goto et al., 2018). For these simulations, body temperatures were directly given according to the measured values in the experiments, instead of the simulated values by using the thermal network model. The coefficients in the autonomic regulation model were determined by tuning to reduce the gaps between simulated and measured values.

Table 3. Simulation cases

Case	Air temperature and MRT	Posture	RH (not controlled)	Air velocity	Clothing insulation
28°C-supine (basic)	28°C	Supine	41±19%	< 0.1 m/s	0.06 clo
18°C-supine	18°C	Supine	50±9%		
40°C-supine	40°C	Supine	29±7%		
28°C-standing	28°C	Standing	32±11%		

3 RESULTS AND DISCUSSIONS

Figure 5 shows the comparisons between the measured and simulated values of arterial BFR and cardiac output. Most of the simulated values agreed well with the measured values, and at least all simulated values reproduced the trend of the BFR changes.

Figure 6 shows the comparisons between the measured and simulated BP. In the 18°C-supine case, the simulated BP in upper arm was lower than the measurement, and almost identical to the BP in the basic case. This discrepancy was possibly caused by that the simulation considered only the constriction of arterioles for the vasomotor activity for thermoregulation. Even though the arterioles are the main effector controlling BFR, it is generally considered that sympathetic stimulation arising from body cooling causes the constriction of venous system as well as arterioles (Guyton and Hall, 2005). The constriction of venous system should decrease their compliances; thus, the simulated BP can be improved by incorporating such responses into our model. On the other hand, another discrepancy was found in the systolic BP at ankle in the 40°C-supine. It was caused by that the simulated BP at ankle, i.e. the BP at posterior tibial, was much affected by the frictional pressure loss in the artery due to high blood flow velocity, although the actual blood flow during BP measurement was impended by a cuff. Figure 7 and 8 show the examples of time variations of simulated BP.

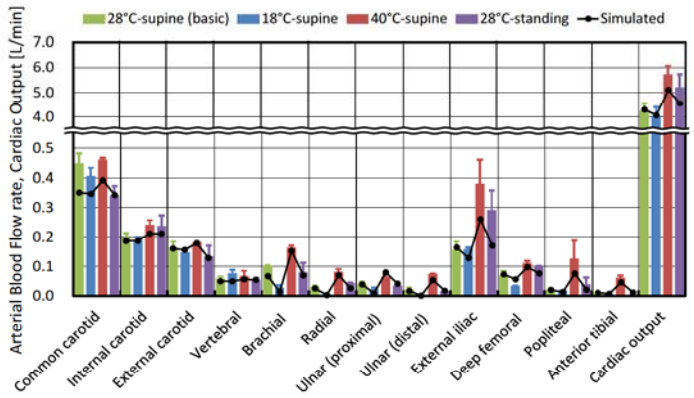

Figure 5. Arterial BFR and cardiac output

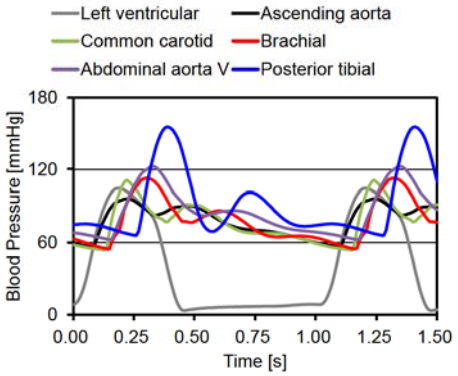

Figure 7. Time variation of simulated BP in 28°C-supine (basic) case

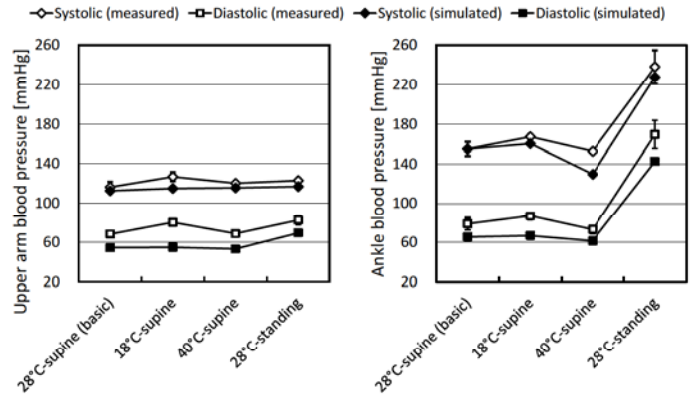

Figure 6. BP at upper arm and ankle

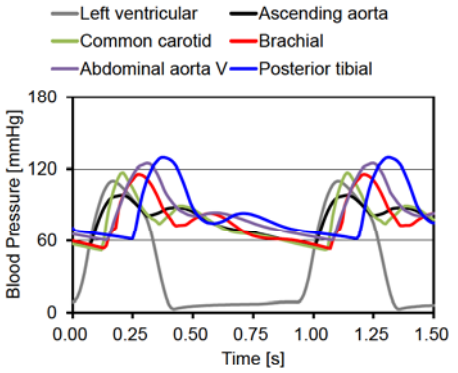

Figure 8. Time variation of simulated BP in 40°C-supine case

4 CONCLUSIONS

We developed a part of the autonomic regulation model such as vasomotor and cardiac activities for thermoregulation and baroreflex, and combined with our cardiovascular model. By comparing with the measurements, we found that the developed model could reasonably

simulate the BP and BFR under four different thermal and postural conditions. Only in the 18°C-supine case, there was a substantial problem on the BP simulation, however, it will be solved by incorporation of more precise vasomotor activity.

5 ACKNOWLEDGEMENT

This work was supported by JSPS KAKENHI (JP16H04460, JP20H02307).

6 NOMENCLATURE

A	cross-sectional area of artery ($=\pi r^2$) [m^2]
A_0	cross-sectional area of artery at reference state (P = 0) [m^2]
B	Bernoulli's resistance of cardiac valve [$Pa \cdot s^2/m^6$]
$BARO$	baroreflex signal
$B_{baro,a}$	coefficient of baroreflex ability (= 1.6)
$B_{baro,s}$	coefficient of sensitivity to BP change (= 0.5)
$B_{dilat,i}$	coefficient of vasodilatation ability of segment i
$B_{stric,i}$	coefficient of vasoconstriction ability of segment i
C	compliance [m^3/Pa]
C_{con}, S_{con}	coefficients of sensitivity to body temperature change for vasoconstriction (= 1.0, 1.0)
C_{dil}, S_{dil}	coefficients of sensitivity to body temperature change for vasodilatation (= 15.6, 1.0)
$DILAT$	integrated thermal stress signal for vasodilatation
E	Young's modulus of artery [Pa]
E_0	zero-volume elastance of pulmonary circulation [Pa/m^3]
E_A	active elastance of heart [Pa/m^3]
E_B	passive elastance of heart [Pa/m^3]
$e(t)$	normalized time-varying elastance of heart [ND]
g	gravitational acceleration [m/s^2]
H	relative height [m]
h	vessel wall thickness [m]
HR	heart rate [beat/s]
L	inertial resistance [$Pa \cdot s^2/m^3$]
P	blood pressure [Pa]
P_{ar}	mean BP of carotid sinus and aortic arch [Pa]
Q	blood flow rate [m^3/s]
R	viscosity resistance [$Pa \cdot s/m^3$]
r	radius of artery [m]
r_0	radius of artery at reference state (P = 0) [m]
S	viscoelastance [$Pa \cdot s/m^3$]
$STRIC$	integrated thermal stress signal for vasoconstriction
t	time [s]
T_{cr}	head core temperature [°C]
$\overline{T}_{sk}$	mean skin temperature [°C]
V	vascular volume [m^3]
$VASO_i$	vasomotor signal for segment i
x	axial coordinate [m]
δ	boundary layer thickness [m]
ν	kinematic viscosity of blood [m^2/s]
ρ	density of blood [kg/m^3]
σ	Poisson's ratio of artery (=0.5) [ND]
Φ	volume constant of pulmonary circulation [m^3]

Subscripts

basic	basic physiological state (thermally neutral and supine condition)
dw	downstream segment adjacent to target segment
i	target segment
set	setpoint
up	upstream segment adjacent to target segment

7 REFERENCES

Goto T, Terayama D, Sugawara R, Sakamoto H. 2017. Parameter quantification for a simulation model of human cardiovascular system. In: *Proceedings of Healthy Buildings Asia*, Tainan, 251-254.

Goto T, Terayama D, Sakamoto H, Hayase T, Saijo Y, Sugawara R, Niu Z. 2018. Development of new human thermal model based on blood flow rate measurements under different temperature conditions, In: *Proceedings of Indoor Air 2018*, Philadelphia, ID202

Guyton AC, Hall JE. 2005. *Textbook of Medical Physiology 11th Edition*, Saunders.

Liang FY, Takagi S, Himeno R, Liu H. 2009. Biomechanical characterization of ventricular-arterial coupling during aging: A multi-scale model study. *Journal of Biomechanics*, 42, 692-704.

Ministry of the environment government of Japan. 2018. *Environmental health manual of heat stroke* (in Japanese).

Sakamoto H, Chiba Y, Hayase T, Funamoto K, Saijo Y, Goto T. 2015. Measurements of blood flow and blood pressure under different indoor temperature and body postural conditions, and development of a new human simulation model. In: *Proceedings of Healthy Buildings Europe*, Eindhoven, ID437.

Stolwijk JAJ. 1971. A mathematical model of physiological temperature regulation in man. NASA contractor report. *NASA contractor report*, NASA CR-1855.

Tokyo metropolitan institute of gerontology. 2013. *Reports of CPA patients in bath room in East Japan* (in Japanese).